Petroleum Science 20 (2023) 2244–2252

Contents lists available at ScienceDirect

Petroleum Science

journal homepage: www.keaipublishing.com/en/journals/petroleum-science

Original Paper

Influence of matrix physical properties on flow characteristics in dual network model

Chen-Chen Wang [a, b], Yong-Fei Yang [c], Deng-Lin Han [b, d], Miao-Miao Su [e], Rong-Rong Hu [f, *]

[a] Cooperative Innovation Center of Unconventional Oil and Gas, Yangtze University, Wuhan, 430100, Hubei, China
[b] Laboratory of Reservoir Microstructure Evolution and Digital Characterization, Yangtze University, Wuhan, 430100, Hubei, China
[c] School of Petroleum Engineering, China University of Petroleum (East China), Qingdao, 266580, Shandong, China
[d] School of Geosciences, Yangtze University, Wuhan, 430100, Hubei, China
[e] College of Resources and Environment, Yangtze University, Wuhan, 430100, Hubei, China
[f] School of Petroleum Engineering, Yangtze University, Wuhan, 430100, Hubei, China

ARTICLE INFO

Article history:
Received 13 January 2023
Received in revised form
12 June 2023
Accepted 18 June 2023
Available online 19 June 2023

Edited by Yan-Hua Sun

Keywords:
Network integration
Dual media
Flow characteristics
Matrix pore density
Matrix filling domain

ABSTRACT

The tight oil formation develops with microfractures and matrix pores, it is important to study the influence of matrix physical properties on flow characteristics. At first, the representative fracture and matrix samples are selected respectively in the dual media, the fracture and matrix digital rocks are constructed with micro-CT scanning at different resolutions, and the corresponding fracture and matrix pore networks are extracted, respectively. Then, the modified integration method is proposed to build the dual network model containing both fracture and matrix pore-throat elements, while the geometric-topological structure equivalent matrix pores are generated to fill in the skeleton domain of fracture network, the constructed dual network could describe the geometric-topological structure characteristics of fracture and matrix pore-throat simultaneously. At last, by adjusting the matrix pore density and the matrix filling domain factor, a series of dual network models are obtained to analyze the influence of matrix physical properties on flow characteristics in dual-media. It can be seen that the matrix system contributes more to the porosity of the dual media and less to the permeability. With the decrease in matrix pore density, the porosity/permeability contributions of matrix system to dual media keep decreasing, but the decrease is not significant, the oil–water co-flow zone decreases and the irreducible water saturation increases, and the saturation interval dominated by the fluid flow in the fracture keeps increasing. With the decrease in matrix filling domain factor, the porosity/permeability contributions of matrix system to dual media decreases, the oil–water co-flow zone increases and the irreducible water saturation decreases, and the saturation interval dominated by the fluid flow in the fracture keeps increasing. The results can be used to explain the dual-media flow pattern under different matrix types and different fracture control volumes during tight oil production.

1. Introduction

Tight oil reservoir has been the key target of oil exploration and development in China. The tight oil formation develops with microfractures and micropores, which results in strong microscopic heterogeneity and forms the fracture-matrix dual media system. Due to the complex matrix pore structure, the oil–water microscopic flow mechanism in tight formation is different from that in conventional formations. It is very important to accurately characterize the matrix pore structure and the influence of its physical properties on flow characteristics in the fracture-matrix dual media (Yang et al., 2011; Cai et al., 2013; Qu et al., 2017).

Since Fatt (1956) introduced the network model, the pore network model has become an important platform for microscopic flow characterization (Hou et al., 2005, Hou et al., 2008; Wang et al., 2005; Xie et al., 2005; Tao et al., 2007). The pore network model can reproduce the complex pore space and simulate the microscopic flow in the extracted pore network model, which not only can reduce the experimental cost and shorten the experimental data

* Corresponding author.
E-mail address: hurongrong87@126.com (R.-R. Hu).

https://doi.org/10.1016/j.petsci.2023.06.006

period, but also can acquire the experimental data that are difficult to measure in the laboratory. In response to the heterogeneous and multi-scale characteristics of the formation space, many scholars have studied multi-scale pore network construction method in recent years. Moctezuma et al. (2003) described the pore space system in cavernous formations by introducing a regular network model with primary bedrock pores and secondary cavern pores, and further elucidated the connectivity between cavern pores and the connectivity characteristics between bedrock pores, the model could characterize the bimodal distribution of pore size and fit the experimental data (porosity, permeability, and capillary force curves, etc.) well for this type of carbonate rocks. Jiang et al. (2012, 2013) proposed a method for integrating pore networks based on scanned rock images at different resolutions, the equivalent pore network models of arbitrary volumes are generated by stochastic modelling based on high resolution images, the network models describing both macropores and micropores are produced by adding links between different scale networks. Mehmani and Prodanovic (2014) and Prodanović et al. (2015) introduced a similar network fusion approach which focused on the distribution areas of micropores, and they used a more specific approach to generate micropore areas by refining the macropore network, the dual pore network model can be used to analyze the basic two-phase flow characteristics of multi-scale cores, and elucidate the fluid flow characteristics in different systems of micropores and macropores. de Vries et al. (2017) assumed that the microscopic aggregate domain contains a large number of micropores to construct a multiscale pore network, these aggregate domains were randomly generated and assigned to macropore domains, the effect of the aggregate parameters (porosity and permeability) on the dual-porosity pore network is then analyzed, it is found that the increase in aggregate porosity can cause considerable tailing in the breakthrough curves; as the permeability of the aggregates increases, it leads to a change in flow from diffusion-dominated to advection-dominated.

Morever, the microfracture network is studied for multi-scale network models. Hughes and Blunt (2001) developed a pore-scale network model of wetting in a fracture, and a variable fracture aperture distribution is represented as a square lattice of conceptual pores connected by throats. Jiang et al. (2017) presented a pore network extraction method with an efficient shrinking algorithm for fractured rocks, and the extraction method is validated to be accurate, efficient and robust for fractured rocks. Han et al. (2021) determined the aperture of fractures and radius of micropores with micro-CT *in-situ* scanning at different confining pressures, and analyzed the stress sensitivity and its main control mechanism. In this paper, based on the modified integration method of pore network, the representative fracture network and pore network are integrated to construct a dual network model containing both fracture and matrix pore/throat, which can describe the geometric-topology structure characteristics of fracture and matrix pore/throat simultaneously. By adjusting the matrix pore density and matrix filling domain factor, respectively, a series of dual-media network models are acquired and the effect of matrix physical properties on the flow characteristics in the water-wet dual media is then analyzed.

2. Methodology

2.1. Digital rock construction

With the advantage of 3D imaging and non-destructive testing, micro-CT produces conical X-rays to penetrate the object, magnifies the image through different magnifications of the objective, and reconstructs a 3D model from the large number of X-ray attenuated images by 360° rotation.

In this paper, micro-CT scanning is used to obtain the representative 3D gray-scale images of dual-media fracture samples and matrix samples, respectively. As shown in Fig. 1a, the 3D gray image of fracture sample is acquired by micro-CT scanning with a voxel resolution of 2 μm, voxel size of 600 × 600 × 600 and physical size of 1200 μm × 1200 μm × 1200 μm. As shown in Fig. 1b, the 3D gray image of matrix sample is acquired by micro-CT scanning with a voxel resolution of 1.5 μm, voxel size of 500 × 500 × 500, and physical size of 750 μm × 750 μm × 750 μm.

Based on the 3D gray image obtained by CT scanning, the image is segmented with watershed algorithm. Watershed segmentation method is based on mathematical morphology in topology theory, which considers the 3D image as a topological landform in geodesy, where the gray value of each voxel in the image represents the altitude of the voxel, and each local minimal value and its influence area is called a catchment basin, and the watershed of the image is obtained by calculating the boundary of the catchment basin.

It can be seen that, the physical meaning of the watershed is to obtain the maximum point of the input image. Therefore, the gradient image is usually used as input to obtain the edge information of the 3D image, that is, the watershed calculation formula is as follows:

$$g(x,y,z) = \mathbf{grad}(f(x,y,z)) \tag{1}$$

where $f(x,y,z)$ denotes the original image and **grad**() denotes the gradient operation.

As shown in Fig. 2, according to the 3D gray images of fracture samples and matrix samples obtained by micro-CT scanning, the corresponding 3D digital cores of fracture and matrix samples were obtained by binary segmentation through watershed algorithm.

2.2. Dual network integration

In this paper, the thinning method is used to extract the pore network model, which mainly includes 3D Euclidean distance map calculation, clustering of voxels, extraction of pore space and pore/throat partitioning (Jiang et al., 2012, 2013). While the fracture system is regarded as a series of "quasi-pores" and "quasi-throats" with well connectivity, and the fracture network can be extracted by the thinning method. Based on 3D digital rock of fracture sample and matrix sample, the corresponding fracture network and matrix pore network model are extracted respectively.

As shown in Fig. 3a, the fracture network model is extracted with physical size of 1200 μm × 1200 μm × 1200 μm. As shown in Fig. 3b, the matrix pore network model is extracted with physical size of 750 μm × 750 μm × 750 μm.

The modified integration method is proposed to build the dual network model containing both fracture and matrix pore/throat in dual media (Jiang et al., 2013). The dual network is produced by generating the geometric-topology equivalent matrix pores/throats in the fracture network model. The specific steps are as follows:

(1) Determining the filling domain of matrix pores in a dual network model. The spatial domain of fracture network model Ω is taken as that of dual network model, and the skeleton domain of fracture network is regarded as the filling domain of matrix pores. Assuming the domain occupied by fractures in fracture network model is Ω_F, the filling domain of the matrix pores could be described as:

$$\Omega_M = \Omega - \Omega_F \tag{2}$$

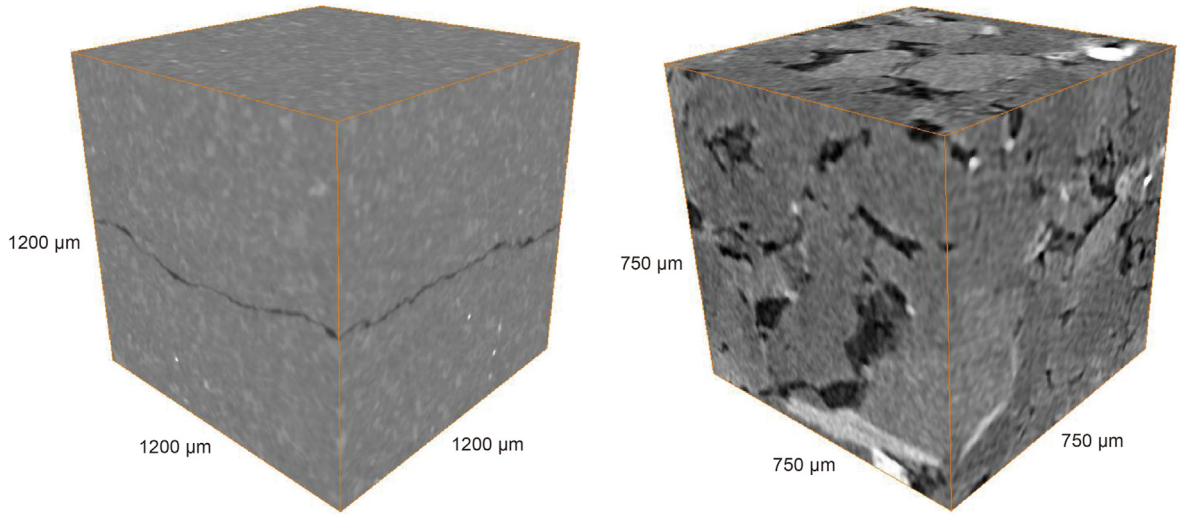

(a) Fracture sample (resolution: 2 μm/voxel) **(b)** Matrix sample (resolution: 1.5 μm/voxel)

Fig. 1. 3D gray image based on micro-CT scanning.

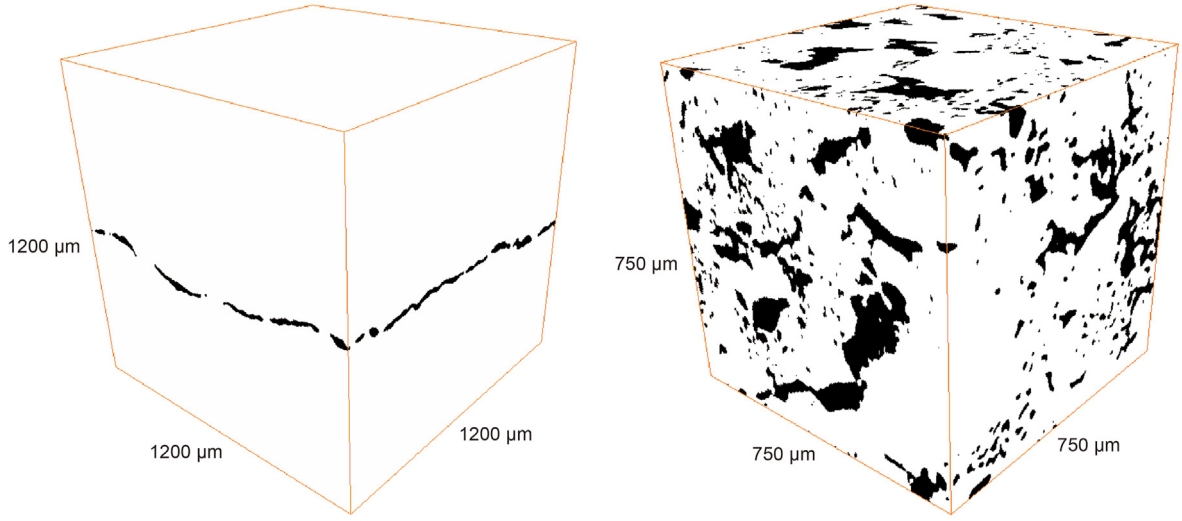

(a) Fracture sample (resolution: 2 μm/voxel) **(b)** Matrix sample (resolution: 1.5 μm/voxel)

Fig. 2. Construction of 3D digital rock.

(2) Generating matrix pores in filling domain with the geometric-topology structure equivalent to that of the original matrix pore network model. According to the statistical analysis of randomly generated pore radius, volume, shape factor and so on, the probability distribution of each variable is consistent with the original matrix pore network model.

The number of pores generated in the filling domain of dual network can be obtained by the definition of scale variation factor:

$$N'_{\mathrm{pm}} = \xi \cdot N_{\mathrm{pm}} \tag{3}$$

where N_{pm} is the number of pores in the original matrix pore network model; ξ is the scale variation factor, that is, the ratio of the equivalent matrix pore filling domain volume to the original matrix pore network volume.

During the process of dual network integration, the matrix pore density α is introduced to improve the construction speed and save storage space:

$$N''_{\mathrm{pm}} = \alpha \cdot N'_{\mathrm{pm}} \tag{4}$$

(3) Adding throats to connect equivalent matrix pores. In the filling domain of matrix pores, geometric-topology structure equivalent matrix pore network is produced by adding throats between matrix pores. While the connectivity function of equivalent matrix pore network with adding throat is consistent with that of the original matrix pore network.

(4) Adding throats between the fracture "quasi-pores" and matrix pores to integrate the dual network. The connection throats between the fracture "quasi-pores" and their adjacent matrix pores are added based on the coordination number distribution of matrix pores.

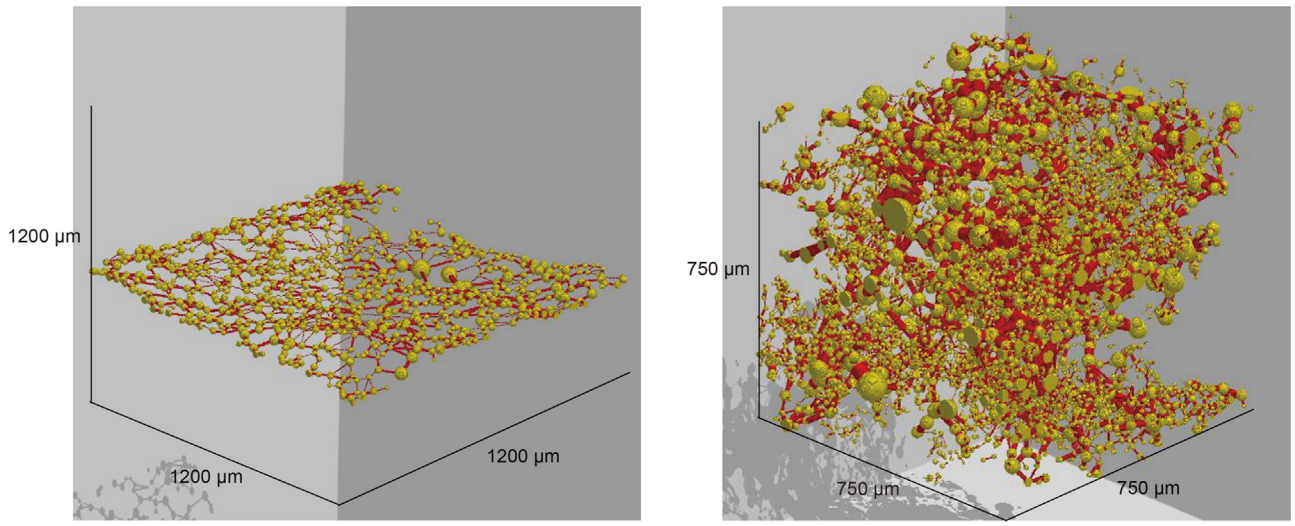

(a) Fracture network model **(b)** Matrix pore network model

Fig. 3. Extraction of 3D network model.

As shown in Fig. 4, through the above steps, the dual network can be constructed with the integration of fracture and matrix pore network in dual media. The dual network can describe the geometric-topological structure characteristics of fractures and matrix pore/throat simultaneously, which greatly increases the diversity and accuracy of the dual network model.

3. Results and discussion

Based on the dual network, the physical properties of matrix and dual network model could be calculated, respectively. Also, the oil–water two-phase flow can be simulated with intrusion–percolation theory, the flow is completely controlled by capillary pressure, and the dual network model can be used to simulate the process of primary drainage and imbibition (Blunt, 2001; Valvatne and Blunt, 2004; Valvatne et al., 2005; Yao et al., 2007; Yang et al., 2015, 2019; Cai et al., 2022). By adjusting the matrix pore density and matrix filling domain factor, a series of dual network models are obtained to analyze the influence of matrix physical properties on flow characteristics in water-wet dual-media.

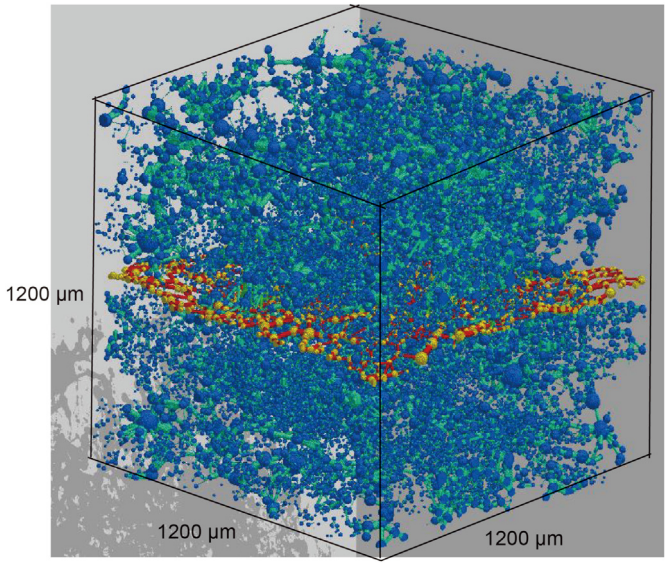

Fig. 4. Integration of fracture and matrix pore network in dual media.

3.1. Influence of matrix pore density

As shown in Table 1, Figs. 5 and 6, different matrix pore densities α are selected to construct the corresponding dual network models, the physical properties of dual media are described based on the network model, and the porosity/permeability rates of matrix system to dual media under different matrix pore densities are compared and analyzed. It can be found that, the matrix system contributes more to the pore/throat numbers of dual media, also, the matrix system contributes more to the porosity and less to the permeability of dual media. With the decrease in matrix pore density, the porosity/permeability contribution of matrix system to dual media keeps decreasing, but the decrease is not significant, the porosity rate keeps 70%–88%, and the permeability rate keeps 1%–12%.

As shown in Fig. 7, oil–water primary drainage and imbibition process of water-wet dual network with different matrix pore densities is simulated, the corresponding capillary pressure curve and relative permeability curve are calculated to show the influence of matrix pore density on flow characteristics of dual media.

As can be seen from primary drainage relative permeability curve at $\alpha = 0.8$, the water saturation S_w ranges from 1 to 0.25 with oil displacement. When $S_W = 1–0.81$, at the initial stage of oil displacement, oil enters the fracture at first as a non-wetting phase and occupies the central area of fracture, and the water relative permeability curve decreases rapidly, at this time, the oil phase has not formed a continuous phase, the oil relative permeability curve shows very little rise; then, as the oil saturation continues to rise, the oil phase forms a continuous phase in the fracture, the oil relative permeability curve rises rapidly. The variations of oil/water relative permeability curves in this interval are mainly dominated by fluid flow in the fracture. When $S_W = 0.81–0.25$, with the continuous oil displacement, oil enters the matrix from the fracture, and the change of fluid saturation mainly reflects the fluid flow characteristics in the matrix. Due to the low permeability of matrix, the oil/water relative permeability curves show gentle

Table 1
Structure comparison with different matrix pore densities.

Matrix pore density α	Matrix pore number	Matrix throat number	Dual network (quasi)pore number	Dual network (quasi) throat number
0.8	20709	19483	21531	20690
0.4	13995	9248	14817	10455
0.2	6853	5921	7675	7128

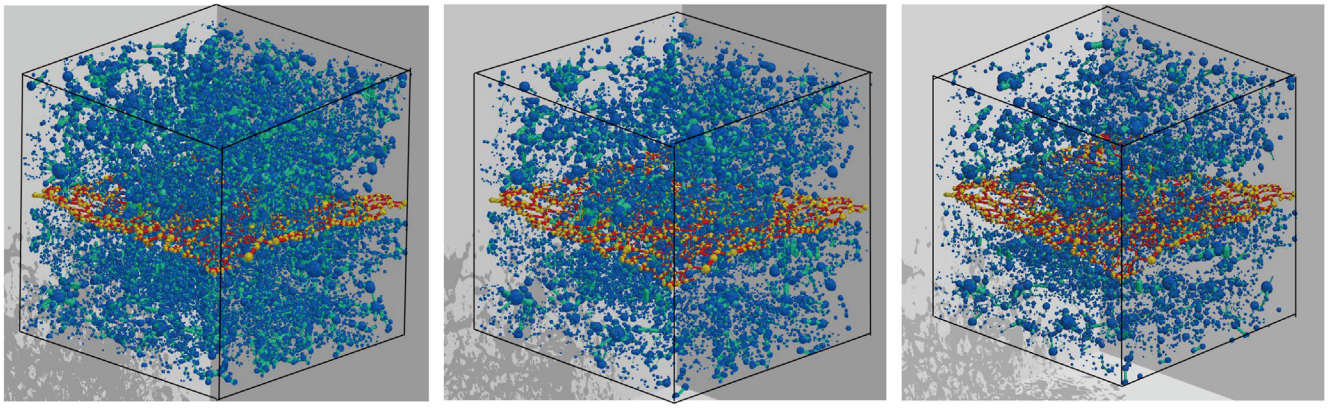

Fig. 5. Dual network with different matrix pore densities.

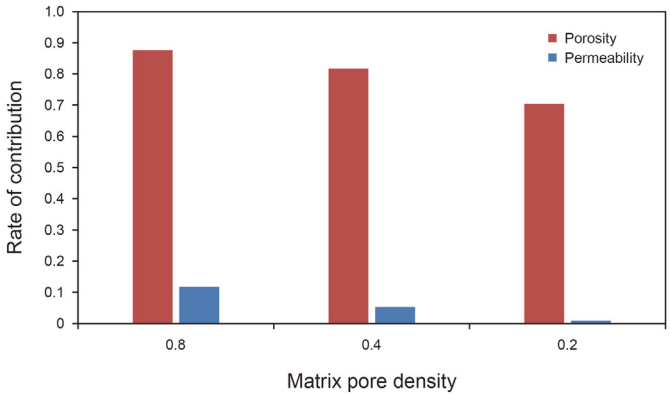

Fig. 6. Porosity/permeability rates of matrix system to dual media under different matrix pore densities.

change. The variations of oil/water relative permeability curves in this interval are mainly dominated by fluid flow from fracture to matrix.

As can be seen from imbibition relative permeability curve at $\alpha = 0.8$, the water saturation S_w ranges from 0.25 to 0.7 with water flooding. When $S_W = 0.25–0.4$, at the initial stage of the water flooding, water enters the fracture at first as the wetting phase and flows along the fracture edge; with the continuous increase in water saturation, the water changes from discontinuous to continuous phases, the water relative permeability curve rises rapidly, while the oil relative permeability curve decreases rapidly. The variations of the oil/water relative permeability curves in this interval are mainly dominated by the fluid flow in the fracture. When $S_W = 0.4–0.7$, with the continuous water flooding, the water saturation increases and it mainly reflectes the cross flow from fracture to matrix. Due to the low permeability of matrix, the oil/water relative permeability curves show gentle change. The variations of oil/water relative permeability curves in this interval are mainly dominated by fluid flow from fracture to matrix.

Totally speaking, with the decrease in matrix pore density from 0.8 to 0.2, the oil–water co-flow zone decreases and the irreducible water saturation increases from 0.25 to 0.6, at the same time, the saturation interval dominated by the fluid flow in the fracture keeps increasing. During the primary drainage process, the water saturation at the inflection point of oil relative permeability curve from fracture-dominated to matrix-dominated keeps shifting to the left from 0.81 to 0.71; while during the imbibition process, the water saturation at the inflection point of water relative permeability curve from fracture-dominated to matrix-dominated keeps shifting to the right from 0.41 to 0.88. This is because the proportion of matrix pores decreases with the decrease in matrix pore density, the connectivity of matrix pores becomes worse and the overall connectivity in dual media decreases. Meanwhile, the proportion of matrix porosity to total porosity decreases, and the proportion of fracture porosity to total porosity continuously rise due to its high connectivity. This can be used to explain the dual-media flow pattern under different matrix types in the oil production process.

3.2. Influence of matrix filling domain

Based on the original filling domain of matrix pores Ω_M, filling domain factor β is introduced to adjust different filling domain of matrix pores, which could be described as follows:

$$\Omega_M^{'} = \beta \cdot \Omega_M \tag{5}$$

As shown in Figs. 8–10 and Table 2, different matrix filling domain factor β are selected to construct the corresponding dual media network model, the physical properties of dual media are calculated based on the network model, the porosity/permeability rates of matrix system to dual media under different matrix filling domain factors are compared and analyzed. It can be found that, the matrix system contributes more to the pore/throat numbers of dual media, also, the matrix system contributes more to the porosity and less to the permeability of the dual media. The porosity/permeability contributions of matrix system to dual media decrease with

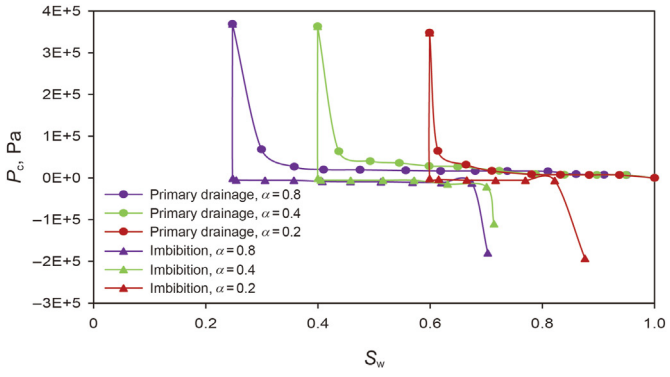

(a) Capillary pressure curve

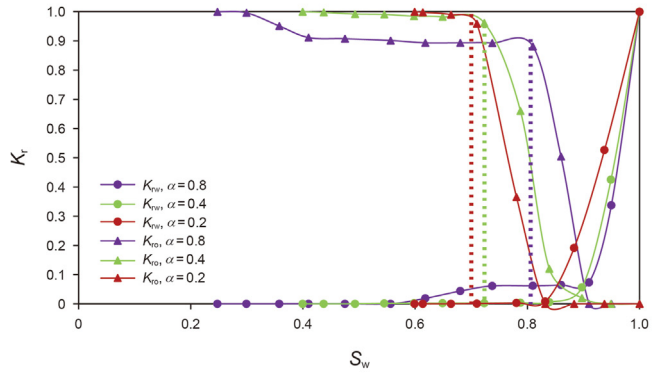

(b) Primary drainage relative permeability curve

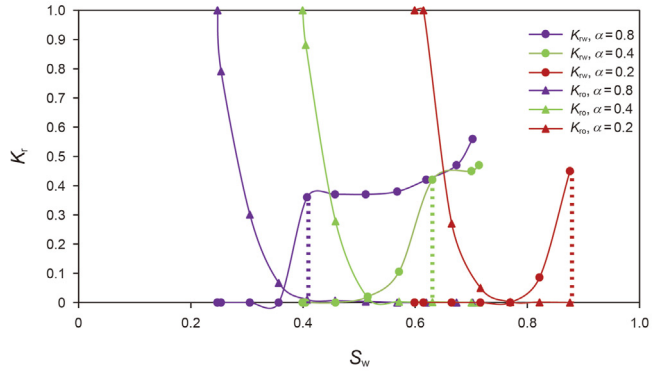

(c) Imbibition relative permeability curve

Fig. 7. Two-phase flow simulation of dual network with different matrix pore densities.

the decrease in matrix filling domain factor, the porosity rate keeps 64%–87%, and the permeability rate keeps 15%–36%.

As shown in Fig. 11, oil–water primary drainage and imbibition processes of water-wet dual network with different matrix filling domain factors are simulated, the corresponding capillary pressure curve and relative permeability curve are calculated to show the influence of matrix filling domain factor on flow characteristics of dual media.

As can be seen from primary drainage relative permeability curve at $\beta = 0.8$, the water saturation S_W ranges from 1 to 0.16 with oil displacement. When $S_W = 1–0.68$, at the initial stage of oil displacement, oil enters the fracture at first as a non-wetting phase and occupies the central area of fracture, and the water relative permeability curve decreases rapidly, at this time, oil phase has not formed a continuous phase, the oil relative permeability curve shows very little rise; then, as the oil saturation continues to rise, the oil phase forms a continuous phase in the fracture, the oil phase relative permeability curve rises rapidly. The variations of oil/water relative permeability curves in this interval are mainly dominated by fluid flow in the fracture. When $S_W = 0.68–0.16$, with the continuous oil displacement, oil enters the matrix from the fracture, and the change of fluid saturation mainly reflects the fluid flow characteristics in the matrix. Due to the low permeability of matrix, the oil/water relative permeability curves show gentle change. The variations of oil/water relative permeability curves in this interval are mainly dominated by fluid flow from fracture to matrix.

As can be seen from imbibition relative permeability curve at $\beta = 0.8$, the water saturation S_W ranges from 0.16 to 0.72 with water flooding. When $S_W = 0.16–0.44$, at the initial stage of the water flooding, water enters the fracture at first as the wetting phase and flows along the fracture edge; with the continuous increase in water saturation, the water changes from discontinuous to continuous phases, the water relative permeability curve rises rapidly, while the oil relative permeability curve decreases rapidly. The variations of the oil/water relative permeability curves in this interval are mainly dominated by the fluid flow in the fracture. When $S_W = 0.44–0.72$, with the continuous water flooding, the water saturation increases and it mainly reflectes the cross flow from fracture to matrix. Due to the low permeability of matrix, the oil/water relative permeability curves show gentle change. The variations of oil/water relative permeability curves in this interval are mainly dominated by fluid flow from fracture to matrix.

Totally speaking, with the decrease in matrix filling domain factor from 0.8 to 0.2, the oil–water co-flow zone increases and the irreducible water saturation decreases from 0.16 to 0.08, at the same time, the saturation interval dominated by the fluid flow in the fracture keeps increasing. During the primary drainage, the water saturation at the inflection point of oil relative permeability curve from fracture-dominated to matrix-dominated keeps shifting to the left from 0.68 to 0.32; while in the imbibition process, the water saturation at the inflection point of water relative permeability curve from fracture-dominated to matrix-dominated keeps shifting to the right from 0.45 to 0.63. This is because the proportion of matrix pores decreases with the decrease in matrix filling domain factor, the connectivity of matrix pores remains constant and the overall connectivity in dual media increases. Meanwhile, the proportion of matrix porosity to total porosity decreases, and the proportion of fracture porosity to total porosity continuously rises due to its high connectivity. This can be used to explain the dual-media flow pattern under different fracture control volumes during oil production.

4. Conclusions

(1) Based on the fracture and matrix pore digital rock, the corresponding fracture network and matrix pore network are extracted, respectively. The modified integration method is introduced to build the dual network model in dual media containing both fracture and matrix pore-throat elements, which could describe the geometric-topological structure characteristics of fracture and matrix pore/throat simultaneously.

(2) By adjusting the matrix pore density and matrix filling domain factor, a series of dual network models are obtained to analyze the influence of matrix physical properties on flow characteristics in water-wet dual-media. It can be found that, the matrix system contributes more to the pore/throat numbers of dual media, also, the matrix system contributes

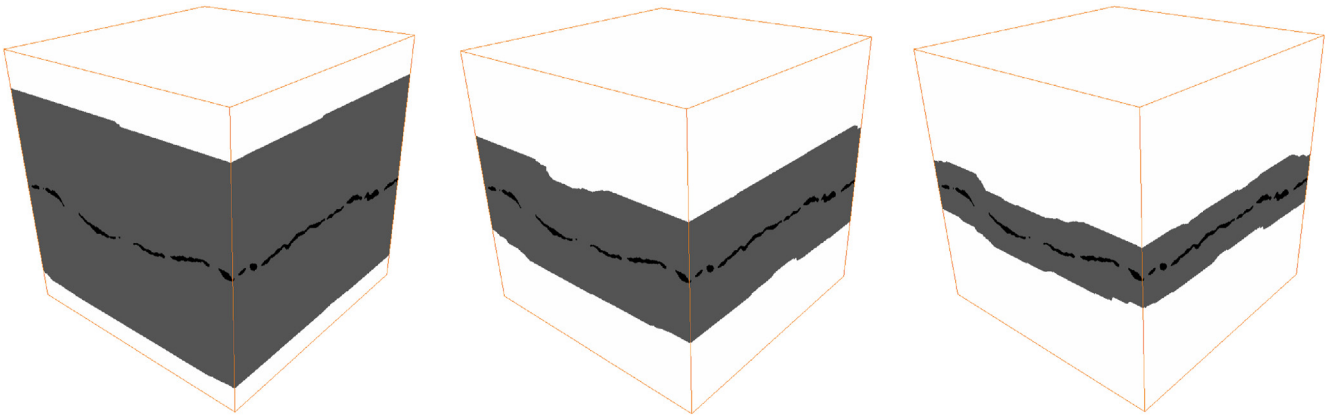

Fig. 8. Different matrix filling domain factors.

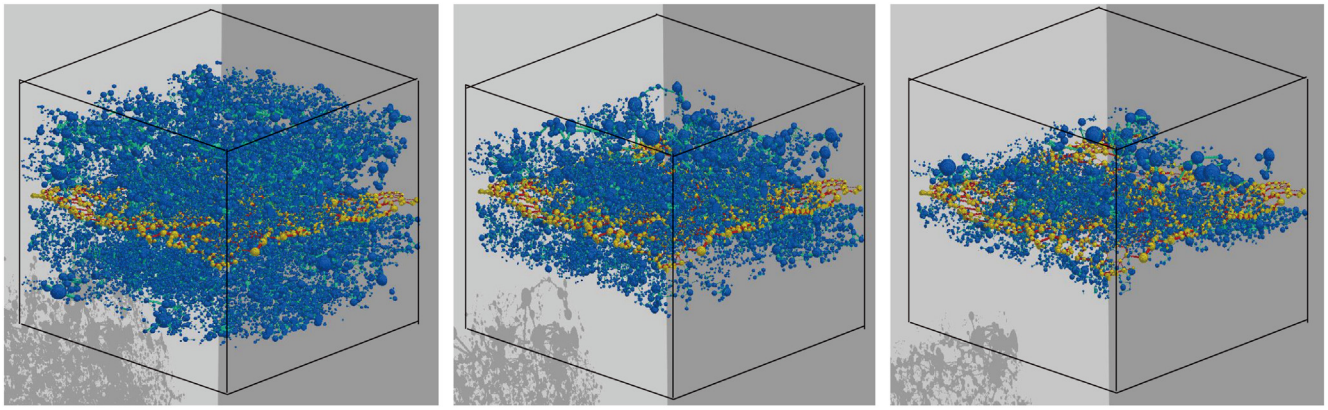

Fig. 9. Dual network with different matrix filling domain factors.

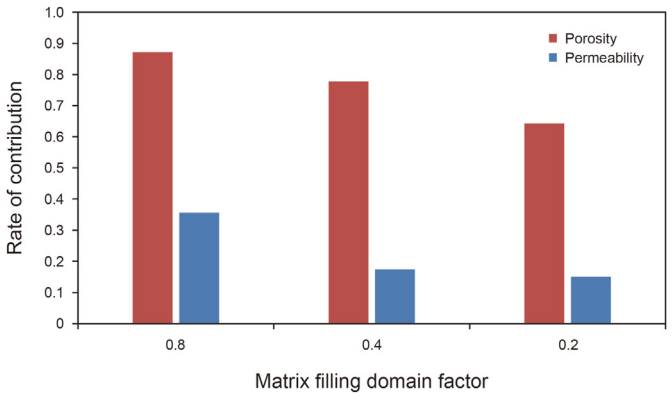

Fig. 10. Porosity/permeability rates of matrix system to dual media under different matrix filling domain factors.

more to the porosity and less to the permeability of dual media. With the decrease in matrix pore density, the porosity/permeability contributions of matrix system to dual media keeps decreasing, but the decrease is not significant, the porosity rate keeps 70%–88%, and the permeability rate keeps 1%–12%. The porosity/permeability contributions of matrix system to dual media decrease with the decrease inf matrix filling domain factor, the porosity rate keeps 64%–87%, and the permeability rate keeps 15%–36%.

(3) With the decrease in matrix pore density from 0.8 to 0.2, the oil–water co-flow zone decreases and the irreducible water saturation increases from 0.25 to 0.6, at the same time, the saturation interval dominated by the fluid flow in the fracture keeps increasing. In the primary drainage process, the water saturation at the inflection point of oil relative permeability curve from fracture-dominated to matrix-

Table 2
Structure comparison with different matrix filling domain factors.

Matrix filling domain factor β	Matrix pore number	Matrix throat number	Dual network (quasi) pore number	Dual network (quasi) throat number
0.8	20844	23568	21666	24775
0.4	11344	12780	12166	13987
0.2	6383	7085	7205	8292

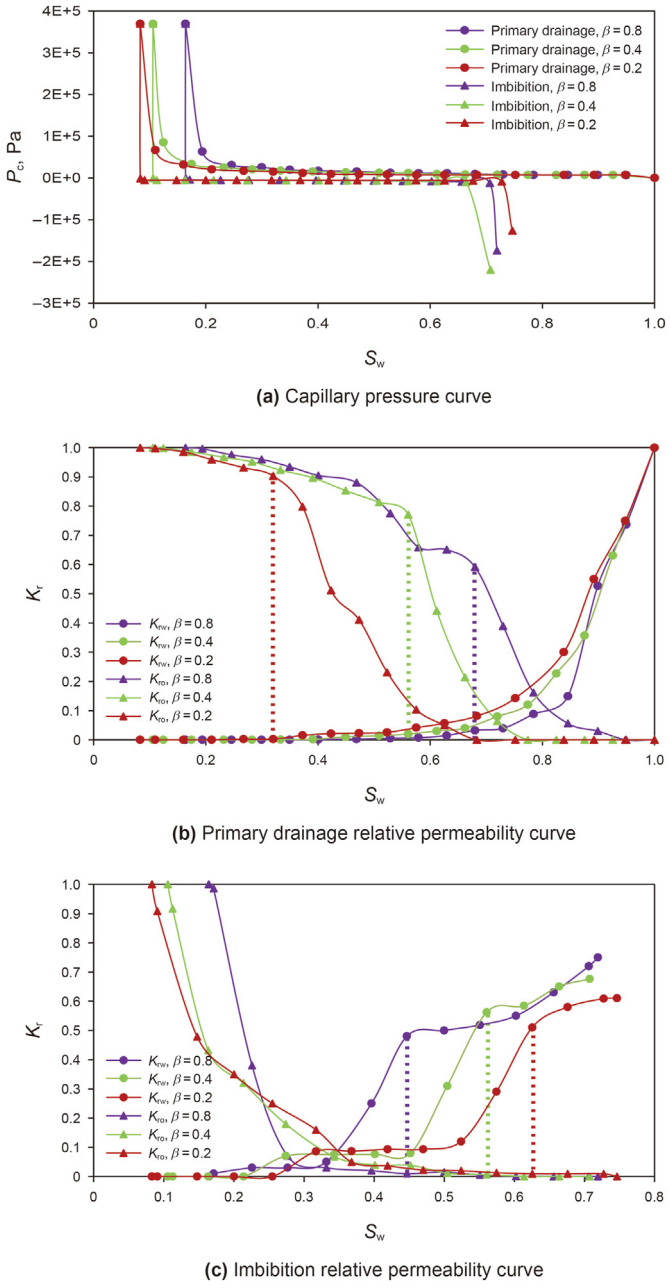

Fig. 11. Two-phase flow simulation of dual media network with different filling domain factors.

dominated keeps shifting to the left from 0.81 to 0.71; while in the imbibition process, the water saturation at the inflection point of water relative permeability curve from fracture-dominated to matrix-dominated keeps shifting to the right from 0.41 to 0.88. This is because the proportion of matrix pores decreases with the decrease in matrix pore density, the connectivity of matrix pores becomes worse and the overall connectivity in dual media decreases. Meanwhile, the proportion of matrix porosity to total porosity decreases, and the proportion of fracture porosity to total porosity continuously rises due to its high connectivity. This can be used to explain the dual-media flow pattern under different matrix types during oil production.

(4) With the decrease in matrix filling domain factor from 0.8 to 0.2, the oil–water co-flow zone increases and the irreducible water saturation decreases from 0.16 to 0.08, at the same time, the saturation interval dominated by the fluid flow in the fracture keeps increasing. In the primary drainage process, the water saturation at the inflection point of oil relative permeability curve from fracture-dominated to matrix-dominated keeps shifting to the left from 0.68 to 0.32; while in the imbibition process, the water saturation at the inflection point of water relative permeability curve from fracture-dominated to matrix-dominated keeps shifting to the right from 0.45 to 0.63.This is because the proportion of matrix pores decreases with the decrease in matrix filling domain factor, the connectivity of matrix pores remains constant and the overall connectivity in dual media increases. Meanwhile, the proportion of matrix porosity to total porosity decreases, and the proportion of fracture porosity to total porosity continuously rises due to its high connectivity. This can be used to explain the dual-media flow pattern under different fracture control volumes during oil production.

Declaration of competing interest

The authors declare that they have no known competing financial interests or personal relationships that could have appeared to influence the work reported in this paper.

Acknowledgements

This work was supported by National Natural Science Foundation of China (No. 51704033, No. 51804038) and PetroChina Innovation Foundation (No. 2018D-5007-0210).

References

Blunt, M.J., 2001. Flow in porous media —pore-network models and multiphase flow. Curr. Opin. Colloid Interface Sci. 6 (3), 197–207. https://doi.org/10.1016/S1359-0294(01)00084-X.

Cai, J., Guo, S., You, L., Hu, X., 2013. Fractal analysis of spontaneous imbibition mechanism in fractured-porous dual media reservoir. Acta Phys. Sin. 62 (1), 228–232. https://doi.org/10.7498/aps.62.014701 (in Chinese).

Cai, J., Wood, D.A., Hajibeygi, H., Iglauer, S., 2022. Multiscale and multiphysics influences on fluids in unconventional reservoirs: modeling and simulation. Adv. Geo-Energy. Res. 6 (2), 91–94. https://doi.org/10.46690/ager.2022.02.01.

de Vries, E.T., Raoof, A., van Genuchten, M.T., 2017. Multiscale modelling of dual-porosity porous media; a computational pore-scale study for flow and solute transport. Adv. Water Resour. 105, 82–95. https://doi.org/10.1016/j.advwatres.2017.04.013.

Fatt, I., 1956. The network model of porous media. Pet. Trans. AIME 207 (1), 144–159. https://doi.org/10.2118/574-G.

Han, D., Wang, H., Wang, C., Yuan, W., Hu, R., 2021. Differential characterization of stress sensitivity and its main control mechanism in deep pore-fracture clastic reservoirs. Sci. Rep. 11 (1), 7374. https://doi.org/10.1038/s41598-021-86444-3.

Hou, J., Li, Z., Guan, J., Wang, K., Chen, Y., 2005. Water flooding microscopic seepage mechanism research based on the three-dimension network model. Chin. J. Theor. Appl. Mech. 37 (6), 783–787. https://doi.org/10.3321/j.issn:0459-1879.2005.06.016 (in Chinese).

Hou, J., Li, Z., Zhang, S., Cao, X., Song, X., 2008. Experimental and simulation study of rock three-deimention network model construction. Scientia Sincina (Physica, Mechanica & Astronomica) 38 (11), 1563–1575 (in Chinese).

Hughes, R.G., Blunt, M.J., 2001. Network modeling of multiphase flow in fractures. Adv. Water Resour. 24 (3), 409–421. https://doi.org/10.1016/S0309-1708(00)00064-6.

Jiang, Z., van Dijke, M.I.J., Wu, K., Couples, G.D., Sorbie, K.S., Ma, J., 2012. Stochastic pore network generation from 3D rock images. Transport Porous Media 94 (2), 571–593. https://doi.org/10.1007/s11242-011-9792-z.

Jiang, Z., van Dijke, M.I.J., Sorbie, K.S., Couples, G.D., 2013. Representation of multiscale heterogeneity via multiscale pore networks. Water Resour. Res. 49 (9), 5437–5449. https://doi.org/10.1002/wrcr.20304.

Jiang, Z., van Dijke, M.I.J., Geiger, S., Ma, J., Couples, G.D., Li, X., 2017. Pore network extraction for fractured porous media. Adv. Water Resour. 107, 280–289. https://doi.org/10.1016/j.advwatres.2017.06.025.

Mehmani, A., Prodanović, M., 2014. The effect of microporosity on transport

properties in porous media. Adv. Water Resour. 63 (2), 104–119. https://doi.org/10.1016/j.advwatres.2013.10.009.
Moctezuma, A., Bekri, S., Laroche, C., Vizika, O., 2003. A dual network model for relative permeability of bimodal rocks application in a vuggy carbonate. In: Proceedings of the International Symposium of the Society of Core Analysts.
Prodanović, M., Mehmani, A., Sheppard, A.P., 2015. Imaged-based multiscale network modelling of microporosity in carbonates. Geol. Soc. London. Spec. Publ. 406 (1), 95–113.
Qu, X., Fan, J., Wang, C., Zhao, G., Shi, J., 2017. Impact of fracture on water flooding seepage features of chang 7 tight cores in Longdong area, Ordos basin. J. Xi'an Shiyou. Univ. (Natural Sci. Ed.) 32 (5), 55–61. https://doi.org/10.3969/j.issn.1673-064X.2017.05.009 (in Chinese).
Tao, J., Yao, J., Li, A., Zhao, X., 2007. Research on oil and water flow using pore-scale network model. Petrol. Geol. Recovery. Effic. 14 (2), 74–77. https://doi.org/10.3969/j.issn.1009-9603.2007.02.020 (in Chinese).
Valvatne, P.H., Blunt, M.J., 2004. Predictive pore-scale modeling of two-phase flow in mixed wet media. Water Resour. Res. 40 (7), W07406. https://doi.org/10.1029/2003WR002627.
Valvatne, P.H., Piri, M., Lopez, X., Blunt, M.J., 2005. Predictive pore-scale modeling of single and multiphase flow. Transport Porous Media 58 (1–2), 23–41. https://doi.org/10.1007/s11242-004-5468-2.
Wang, K., Guan, J., Fan, Y., Hou, J., Sun, J., 2005. The application of pore scale network model in seepage mechanism. Adv. Mech. 35 (3), 353–360. https://doi.org/10.3321/j.issn:1000-0992.2005.03.006 (in Chinese).
Xie, C., Guan, Z., Jiang, S., 2005. Reservoir pore structure model based on micro-cosmic network stochastic simulation. Bull. Geol. Sci. Technol. 24 (2), 97–100. https://doi.org/10.3969/j.issn.1000-7849.2005.02.017 (in Chinese).
Yang, S., Li, M., Wang, L., Kang, M., Zhang, X., 2011. Producing degree and law of matrix in dual-porosity reservoir. J. China. Univ. Pet., (Ed. Nat. Sci.) 35 (1), 98–101. https://doi.org/10.3969/j.issn.1673-5005.2011.01.019 (in Chinese).
Yang, Y., Yao, J., Wang, C., Ying, G., Song, W., 2015. New pore space characterization method of shale matrix formation by considering organic and inorganic pores. J. Nat. Gas Sci. Eng. 27 (P2), 496–503. https://doi.org/10.1016/j.jngse.2015.08.017.
Yang, Y., Wang, K., Zhang, L., Sun, H., Ma, J., 2019. Pore-scale simulation of shale oil flow based on pore network model. Fuel 251, 683–692. https://doi.org/10.1016/j.fuel.2019.03.083.
Yao, J., Tao, J., Li, A., 2007. Research on oil-water two-phase follow using 3D random network model. Acta Pet. Sin. 28 (2), 94–97. https://doi.org/10.3321/j.issn:0253-2697.2007.02.018 (in Chinese).